Cyclotron-Induced Damping of Gould –Trivelpiece Modes in Plasma Column with Dual Ion Species

Daljeet Kaur[1], Manjeet Kaur[2*], Ruby Gupta[3], Ambika Tundwal[4], Simmi Singh[5]

[1,2,4,5] Department of Applied Sciences, Guru Tegh Bahadur Institute of Technology,Guru Gobind Singh Indraprastha University, New Delhi

[3]Department of Physics, Swami Shraddhanand College, University of Delhi, Alipur, Delhi

[*]Corresponding author

DOI: https://doi.org/10.51584/IJRIAS.2025.1005000109

Received: 03 June 2025; Accepted: 07 June 2025; Published: 20 June 2025

ABSTRACT

Cyclotron damping of Gould –Trivelpiece modes is analysed in this study for a cylindrical plasma column containing either SF_6^- or K^+ ions. The study highlights the contrasting roles of ion polarity in mediating wave–particle interactions that govern damping behaviour. It is observed that negative ions, due to their higher mass and weaker cyclotron resonance, result in reduced damping rates of TG modes. Conversely, positive ions enable stronger cyclotron coupling, leading to enhanced damping through more effective resonance with the wave field. Furthermore, the sensitivity of cyclotron damping rates to plasma electronegativity exhibits opposite trends for negative and positive ion plasmas. These findings underscore the critical influence of ion species and plasma composition on the propagation and attenuation of electrostatic waves in electronegative plasma columns, with implications for wave control and energy dissipation in beam-plasma systems.

Keywords: Cyclotron damping, Beam–plasma interaction, Wave–particle resonance, Gould –Trivelpiece mode, Negative ions (SF_6^-), Positive ions (K^+), Electronegativity dependence Plasma wave attenuation.

INTRODUCTION

TG waves, often referred to as lower hybrid waves (LHWs), represent electrostatic phenomena that exist in the frequency domain lying between the ion plasma and electron cyclotron frequencies. These waves have drawn a lot of theoretical and experimental attention across many decades [1–5] due to their effective capability for heating and energy absorption from electrons, notably observed near the outer region of the plasma.

In confined plasmas, Trivelpiece–Gould (TG) waves are typically characterized by short radial wavelengths, whereas in unbounded plasmas, they manifest as modes with short azimuthal wavelengths [6]. Praburam and Sharma [7] demonstrated that TG waves at higher harmonics can be excited using low-energy electron beams. Using the linear Princeton Q-1 device, Seiler et al. [8] investigated the instability of lower hybrid waves (LHWs) induced by a spiraling ion beam. Similarly, Chang [9] analysed the dynamics of LHW instabilities resulting from the perpendicular injection of ion beams. Sharma et al. [10] explored how a modulated electron beam can excite LHWs in a cylindrical plasma configuration. In a related study, Prakash et al. [11] examined LHW generation by ion beams and reported that the fastest growth rate of instability occurs when the wave's phase velocity, aligned with the magnetic field, closely matches the electron thermal velocity.

Recent studies have expanded to include plasmas containing dust grains [12–17]. Both theoretical and experimental investigations have been carried out in non-magnetized [12] and weakly magnetized [13] dusty plasma environments. Sharma et al. [14] proposed a model in which ion-acoustic waves (IAWs) are excited by ion beams within a magnetized dusty plasma cylinder. Kaur et al. explored the excitation of Gould–Trivelpiece modes in dusty plasmas due to streaming particles, focusing on instability growth rates and wave–particle interactions using a fluid-based approach to describe mode dynamics in the presence of dust. Barkan et al. [16] analysed ion-acoustic waves in magnetized dusty plasmas and observed that the wave phase velocity increases with a higher number density of dust grains. Additionally, Rosenberg [17], employing Vlasov theory, examined

ISSN No. 2454-6194 | DOI: 10.51584/IJRIAS |Volume X Issue V May 2025

the instabilities associated with dust-ion acoustic and dust-acoustic modes in unmagnetized dusty plasmas. Annaratone et al. [18] studied the rotational dynamics of a magnetized plasma in the linear device Mistral. They noted that the injected electrons from a central source travel radially outward because of the Lorentz force exerted by an axial magnetic field. Bettega et al. [19] carried out experimental studies on ion-driven diocotron instabilities in electron plasmas confined within a Malmberg–Penning trap. David [20] offered a comprehensive tomographic analysis of linear magnetized plasmas, focusing on the spatial and temporal characterization of plasma structures. Dem'yanov et al. [21] conducted a foundational investigation into equilibrium conditions and nonlocal ion cyclotron instabilities in plasmas influenced by crossed longitudinal magnetic fields and strong radial electric fields. Dubin [22] offers an in-depth review of the physics governing non-neutral plasmas confined in Penning traps, emphasizing the theory and behaviour of collective oscillation modes.

Fajans [23] investigates a specific class of plasma instabilities that occur in non-neutral plasmas due to the presence of a small population of ions. Jaeger [24] provides an in-depth investigation into low-frequency instabilities that arise in magnetized plasma systems with crossed electric and magnetic fields. Kabantsev and Driscoll [25] presents an important experimental study on instabilities in pure electron plasmas, particularly within Penning–Malmberg traps. Levy, Daugherty, and Buneman[26] analyzes ion-induced instabilities in non-neutral plasmas, particularly focusing on conditions relevant to diocotron mode. Peurrung, Notte, and Fajans The first direct observation of ion resonance instability—a key phenomenon involving resonant interactions between ions and collective plasma oscillations—was reported in [27]. Sakawa and Joshi [28] explored both the growth and nonlinear development of the modified Simon–Hoh instability in plasmas produced by electron beams. Yeliseyev [29] analysed the spectral features of modified ion cyclotron oscillations in non-neutral plasmas formed via gas ionization. Yeliseyev [30] analysed the oscillation spectrum of an electron gas containing a small fraction of ions, revealing how even a minor ion presence can significantly influence the collective oscillation modes. Yeliseyev [31] examined Trivelpiece–Gould modes in conjunction with low-frequency electron-ion instabilities within non-neutral plasmas. Kaur, Sharma, and Pandey [32] studied the excitation of Gould–Trivelpiece (TG) modes by a relativistic electron beam in a magnetized dusty plasma. Their findings highlighted how the interplay between the electron beam and dusty plasma can initiate TG modes, uncovering significant nonlinear phenomena and wave-particle interactions in magnetically influenced complex plasma systems.

In this study, a theoretical model is developed to examine the cyclotron damping of the Gould–Trivelpiece (TG) mode by an electron beam interaction with negative ion and positive ion plasma in a finite cylindrical magnetized plasma. Section 2 presents the instability analysis for interaction with SF_6^- negative ions and K^+ positive ions in finite geometry. The fluid approach is employed to determine the responses of beam electrons, plasma electrons, and plasma ions (SF_6^- negative ions and K^+ positive ions) The expressions for the instability growth rates are derived using first-order perturbation theory. In Section 3, numerical analysis and discussions are given. Comparison with experimental and theoretical works in section 4 and concluding remarks are summarized in Section 5.

Instability Characterization

We examine a cylindrical plasma column of radius a_1 containing negative ions SF_6^-, positive ions K^+, and electrons, with equilibrium densities of electrons, positive ions, and negative ions denoted by $n_{e0} = (1-\varepsilon)n_{p0}$, $n_{+0} = n_{p0}$ and $n_{-0} = n_{p0}$ respectively, where n_{p0} represents the overall plasma density. The electrons have temperature T_e and mass m_e, while the positive ions are characterized by temperature $T_{k^+}(=T_e)$ and mass m_+. Similarly, the negative ions have temperature $T_{SF_6^-}(=T_e)$ and mass m_-. An electrostatic wave, specifically a Gould–Trivelpiece (TG) wave, is considered to propagate at an angle relative to the external magnetic field, with the wave vector k lying in the x–z plane.

This equilibrium is perturbed by an electrostatic disturbance, and the corresponding potential associated with this perturbation is expressed as

ISSN No. 2454-6194 | DOI: 10.51584/IJRIAS |Volume X Issue V May 2025

$$\Phi = \Phi_0 e^{[-i(\omega t - k_x x - k_z z)]}. \quad (1)$$

An electron beam travels along the z-axis, aligned with the external magnetic field, with a uniform density n_{b0}, radius f_b, and equilibrium velocity $\upsilon_{b0}\hat{z}$. Before the introduction of any perturbation, the combined beam–plasma system is assumed to be quasineutral

such that $(-n_{e0} + n_{+0} - n_{-0} - n_{b0} \approx 0)$ here we have taken $n_{p0} >> n_{b0}$.

Each of the three species is modeled as a fluid and obeys the continuity and momentum (equation of motion) equations, expressed as:

$$m_e\left[\frac{\partial \vec{\upsilon}}{\partial t} + (\vec{\upsilon}.\nabla)\vec{\upsilon}\right] = -e\vec{E} - \frac{e}{c}\vec{\upsilon}\times\vec{B} \quad (2)$$

$$\frac{\partial n}{\partial t} + \nabla.(n\vec{\upsilon}) = 0. \quad (3)$$

Upon linearizing the equations of motion and continuity [cf. Eqs. (2) and (3)], the resulting expressions for the perturbations in electron density, positive ion density, and negative ion density are obtained as:

$$n_{1e} = -\frac{(1-\varepsilon)n_{e0}e\phi}{m_e}\left[\frac{-\nabla_\perp^2\phi}{\omega^2 - \omega_{ce}^2} + \frac{k_z^2\phi}{\omega^2}\right], \quad (4)$$

$$n_{+i1} = \frac{\varepsilon n_{p0}e\phi}{m_+}\left[\frac{-\nabla_\perp^2\phi}{\omega_{+c}^2} + \frac{k_z^2\phi}{\omega^2}\right], \quad (5)$$

$$n_{-i1} = \frac{-\varepsilon n_{p0}e}{m_{-i}}\left[\frac{-\nabla_\perp^2\phi}{\omega_{-c}^2} + \frac{k_z^2\phi}{\omega^2}\right], \quad (6)$$

$$n_{eb1} = \frac{n_{eb0}ek_z^2\phi}{m_b(\omega - k_z\upsilon_{b0})^2}. \quad (7)$$

where $\omega_{ce}\left(=\frac{eB}{m_e c}\right)$ is the electron gyro frequency, $\omega_{+ci}\left(=\frac{eB}{m_{+i}c}\right)$ is the positive ion-cyclotron frequency, $\omega_{-ci}\left(=\frac{eB}{m_{-i}c}\right)$ is the negative ion gyro-frequency. Substituting the expression from Eqs. (4), (5), (6) & (7) in Poisson's equation

$\nabla^2\Phi = 4\pi e(n_{1e} + n_{-i1} - n_{+i1} + n_{eb1})$ and solving for finite geometry

$(\nabla^2\Phi = \nabla_\perp^2\Phi + \nabla_z^2\Phi = \nabla_\perp^2\Phi - k_z^2\Phi)$ *we will get*

$$\nabla_\perp^2\Phi + \left(\frac{\omega^2 + \omega_{+pi}^2(1-\varepsilon) + \omega_{pe}^2 + \omega_{-pi}^2\varepsilon}{\omega^2\alpha}\right)k_z^2\Phi = \frac{\omega_{pb}^2k_z^2}{\alpha(\omega - k_z\upsilon_{b0})^2} \quad (8)$$

ISSN No. 2454-6194 | DOI: 10.51584/IJRIAS |Volume X Issue V May 2025

where $\omega_{pe}=\left(\frac{4\pi n_{e0}e^2}{m_e}\right)^{1/2}$, $\omega_{+pi}=\left(\frac{4\pi n_{+i0}e^2}{m_+}\right)^{1/2}$, $\omega_{-pi}=\left(\frac{4\pi n_{-i0}e^2}{m_-}\right)^{1/2}$ *and* $\omega_{pb}=\left(\frac{4\pi n_{b0}e^2}{m_b}\right)^{1/2}$ are the electron, positive ion, negative ion and electron beam frequency. Solving Eq. (8)

where,

$$p_0^2=\frac{\beta}{\alpha} \tag{9}$$

$$\beta=\frac{\omega^2+\omega_{+pi}^2(1-\varepsilon)+\omega_{pe}^2+\omega_{-pi}^2\varepsilon}{\omega^2\alpha}, \quad \alpha=\frac{1-\omega_{+pi}^2(1-\varepsilon)}{\omega_{+ci}^2}-\frac{\omega_{pe}^2}{(\omega^2-\omega_{ce}^2)}+\frac{\omega_{-pi}^2\varepsilon}{\omega^2}$$

$$\frac{\partial^2\Phi}{\partial r^2}+\frac{1}{r}\frac{\partial\Phi}{\partial r}+p_0^2\Phi=\frac{\omega_{pb}^2k_z^2\Phi}{(\omega-k_z\upsilon_{b0})^2\alpha} \tag{10}$$

In the absence of the electron beam, Eq. (10) simplifies and can be reformulated as:

$$\frac{\partial^2\Phi}{\partial r^2}+\frac{1}{r}\frac{\partial\Phi}{\partial r}+p_0^2\Phi=0 \tag{11}$$

Equation (11) is recognized as a standard Bessel equation, and its general solution can be expressed as $\Phi=lJ_0(p_dt)+mY_0(p_dt)$, where L and M are arbitrary constants. Here J_0 denotes the zeroth-order Bessel function of the first kind, while Y_0 denotes the zeroth-order Bessel function of the second kind.

At $t=0$, $Y_0\to\infty$ and hence m=0, $\Phi=lJ_0(p_dt)$, $p_0=p_d$. At $t=a_1$, Φ must vanish, hence, $J_0(p_da_1)=0$, $p_d=\frac{X_d}{a_1},(d=1,2,...)$, where X_d represents the zeros of the Bessel function $J_0(X)$. In the presence of the electron beam, the wave function Φ can be expressed as an orthogonal set of eigenfunctions.

$$\Phi=\sum_n AJ_0(p_nt) \tag{12}$$

Further, using the value of Φ in Equation (10) from Equation (12) and multiplying both the sides of Eq.(9) by $tJ_0(p_dt)$ and integrating over t from 0 to a_1, here radius of plasma is a_1, Keeping solely the principal mode n = d we obtain

$$p_0^2-p_d^2=\frac{\omega_{pb}^2k_z^2\sigma}{(\omega-k_z\upsilon_{b0})^2\alpha}, \tag{13}$$

where $\sigma=\dfrac{\int_0^{f_b}tJ_0(p_nt)J_0(p_dt)dr}{\int_0^{a_1}tJ_0(p_nt)J_0(p_dt)dr}$ if $f_b\neq a_1$

=1 if $f_b=a_1$.

Upon substitution of the value of p_0^2 from Eq. (9) in Eq. (13) we obtain,

ISSN No. 2454-6194 | DOI: 10.51584/IJRIAS |Volume X Issue V May 2025

$$1+\frac{\omega^2 k_z^2}{\alpha_2 p_n^2}+\frac{\omega_{+pi}^2(1-\varepsilon)k_z^2}{\alpha_2 p_n^2}+\frac{\omega_{-pi}^2\varepsilon k_z^2}{\alpha_2 p_n^2}-\frac{\omega^2}{\alpha_2}+\frac{\omega_{+pi}^2(1-\varepsilon)\omega^2}{\alpha_2\omega_{+ci}^2}$$
$$-\frac{\omega_{-pi}^2\varepsilon}{\alpha_2}=\frac{\omega_{pb}^2\omega^2 k_z^2}{(\omega-k_z\upsilon_{b0})^2\alpha_2 p_n^2} \quad (14)$$

where , $\alpha_2=\dfrac{\omega_{pe}^2(\omega^2-\omega_{ce}^2)k_z^2+\omega_{pe}^2\omega^2 p_n^2}{(\omega^2-\omega_{ce}^2)p_n^2}$

Now, evaluate Eq. (14) under two conditions: (i) interaction between an electron beam and a plasma that includes negative ions (SF_6^-) and (ii) with positive (K^+) ion.

Case I: Interaction between an electron beam and a plasma that includes negative ions (SF_6^-)

We will reduce Eq. (14) in the absence of positive (K^+) ion to

$$\omega^2-\frac{\omega_{-pi}^2\varepsilon}{\alpha_1\alpha_2}\left[1-\frac{\omega_{-pi}^2 k_z^2}{p_n^2}\right]=\frac{\omega_{pb}^2\omega^2 k_z^2}{(\omega-k_z\upsilon_{b0})^2\alpha_1\alpha_2 p_n^2} \quad (15)$$

where, $\alpha_1=\dfrac{1}{\alpha_2}\left(\dfrac{k_z^2}{p_n^2}-1\right)$

Eq. (15) can be rewrite as

$$(\omega^2-L^2)=\frac{\omega_{pb}^2\omega^2 k_z^2}{(\omega-k_z\upsilon_{b0})^2\alpha_1\alpha_2 p_n^2}$$

$$(\omega-L)(\omega+L)=\frac{\omega_{pb}^2\omega^2 k_z^2}{(\omega-k_z\upsilon_{b0})^2\alpha_1\alpha_2 p_n^2},$$

where, $L=\left[\dfrac{\omega_{-pi}^2\varepsilon}{\alpha_1\alpha_2}\left(1-\dfrac{k_z^2}{p_n^2}\right)-1\right]^{1/2}$ (16)

When the beam is present, the frequency ω can be expanded as as $\omega=L_1+\Delta_1=k_z\upsilon_{b0}+\Delta_1$, Here, Δ_1 the small frequency deviation arises from the finite term on the right-hand side of Eq. (16). Cyclotron damping is represented by the imaginary part of the frequency, when it is negative due to cyclotron resonance between the wave (e.g., Gould –Trivelpiece mode) and ion gyro-motion.

According to Mikhailovski [32], the growth rate of the unstable mode can be expressed as

$$\Gamma 1=\mathrm{Im}\,\Delta_1=\frac{\sqrt{3}}{2}\left[\frac{\omega_{pb}^2 k_z^2 L_1^2}{\alpha_1\alpha_2 p_n^2}\right]^{1/3}, \quad (17)$$

The real part of the frequency for the unstable mode is expressed as

$$\omega_r=k_z\upsilon_{b0}-\tfrac{1}{2}\left[\frac{\omega_{pb}^2 L_1 k_z^2}{2\alpha_1\alpha_2 p_n^2}\right]^{1/3} \quad (18)$$

ISSN No. 2454-6194 | DOI: 10.51584/IJRIAS |Volume X Issue V May 2025

$$\omega_r = k_z\left[\frac{2eV_b}{m_b}\right]^{1/2} - \tfrac{1}{2}\left[\frac{\omega_{pb}^2 L_1 k_z^2}{2\alpha_1\alpha_2 p_n^2}\right]^{1/3} \tag{19}$$

Case II: Interaction between an electron beam and a plasma that includes positive ion (K^+)

We will reduce Eq. (14) in the absence of negative (SF_6^-) ion to

$$\omega^2 - \left(\frac{\omega_{+pi}^2(\varepsilon-1)k_z^2}{\alpha_2\alpha_3 p_n^2} - \frac{1}{\alpha_3(\varepsilon-1)}\right) = \frac{\omega_{pb}^2\omega^2 k_z^2}{(1-\varepsilon)(\omega-k_z\upsilon_{b0})^2\alpha_3\alpha_2 p_n^2} \tag{20}$$

Further solving Eq. (20) we will get

$$\omega^2 - L_2^2 = \frac{\omega_{pb}^2\omega^2 k_z^2}{(1-\varepsilon)(\omega-k_z\upsilon_{b0})^2\alpha_3\alpha_2 p_n^2} \tag{21}$$

where,

$$\alpha_3 = \frac{k_z^2}{\alpha_2 p_n^2(1-\varepsilon)} - \frac{1}{\alpha_2(1-\varepsilon)} + \frac{\omega_{+pi}^2}{\alpha_2\omega_{+ci}^2}$$ and

$$L_2 = \left(\frac{\omega_{+pi}^2(\varepsilon-1)}{\alpha_2\alpha_3 p_n^2}\right)^{1/2}.$$

By applying a similar procedure as in Case I, the growth rate of the unstable mode can be expressed as

$$\Gamma_2 = \mathrm{Im}\,\Delta_2 = \frac{\sqrt{3}}{2}\left[\frac{\omega_{pb}^2 k_z^2 L_2^2}{2\alpha_2\alpha_3(1-\varepsilon)p_n^2}\right]^{1/3}, \tag{22}$$

The real part of the frequency for the unstable mode is expressed as

$$\omega_r = k_z\upsilon_{b0} - \tfrac{1}{2}\left[\frac{\omega_{pb}^2 L_1 k_z^2}{2\alpha_1\alpha_2 p_n^2}\right]^{1/3} \tag{23}$$

$$\omega_r = k_z\left[\frac{2eV_b}{m_b}\right]^{1/2} - \tfrac{1}{2}\left[\frac{\omega_{pb}^2 L_1 k_z^2}{2\alpha_1\alpha_2 p_n^2}\right]^{1/3}. \tag{24}$$

In both cases, the real part of the unstable mode's frequency increases with the beam voltage, consistent with the experimental findings reported by Chang [33].

Numerical Analysis

For the numerical calculations, we have employed the experimental plasma parameters reported by Song et al. [37]. The plasma density value used is $n_{p0} = n_{i0} = 1\times10^9\,cm^{-3}$, T_e=0.2eV, T_{K^+}= T_e , $T_{SF_6^-}$ = T_e ,

ISSN No. 2454-6194 | DOI: 10.51584/IJRIAS |Volume X Issue V May 2025

$\varepsilon(=n_{SF_6^-}/n_{K^+}) = 0.55, 0.65, 0.75, 0.80, 0.95$. Beam radius =1.2 cm, beam density ranges from $n_{b0} = 5\times10^7\, cm^{-3} - 5\times10^8\, cm^{-3}$, electron beam energy= 30KeV, strength of applied magnetic field B=10^4 Gauss and mode number of Bessel function n=1 (1st zero) . Using Equations (17), we have plotted figure1 the growth rate $\Gamma 1\,(\text{sec}^{-1})$ as a function of the longitudinal wave number (cm^{-1}) for various values of ε , considering the presence of both a negative ion and an electron beam and using Equations (22), we have plotted figure 2 the growth rate $\Gamma 2\,(\text{sec}^{-1})$ as a function of the longitudinal wave number (cm^{-1}) for various values of ε , considering the presence of both a positive ion and an electron beam.

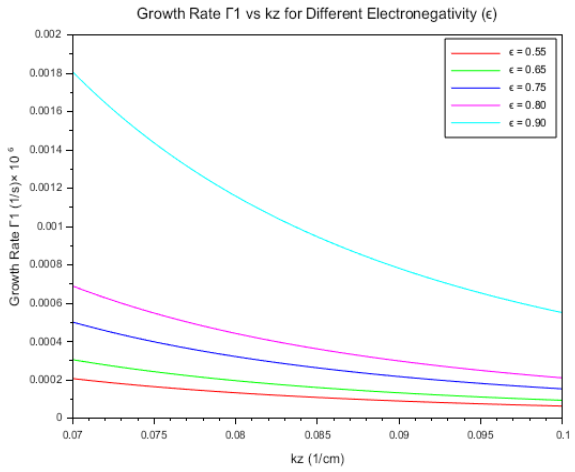

Figure 1: The variation of the growth rate $\Gamma 1$ (s^{-1}) of the unstable TG wave mode with respect to the longitudinal wave number k_z (cm^{-1}) is shown for different values of ε , in the presence of a negative ion and an electron beam

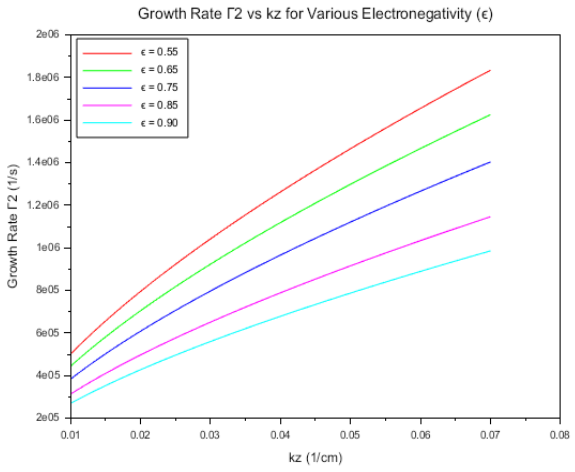

Figure 2: Illustrates the variation in the growth rate $\Gamma 2$ (s^{-1}) of the unstable TG wave mode with respect to the longitudinal wave number k_z (cm^{-1}) for different values of ε , in the presence of a positive ion and an electron beam

The electron beam interaction-induced plasma growth behaviour is quite different based on whether the plasma consists almost entirely of negative ions (like SF_6^-) or positive ions (like K^+). This can be seen from the comparison between the two plots given. In the initial graph (Fig.1), representing the coupling of an electron beam with a plasma with SF_6^- negative ions, the rate of growth ($\Gamma 1$) is seen to reduce with longitudinal wave number k_z (cm^{-1}). In addition, in this cylindrical geometry, the cyclotron damping amplitude of the Trivelpiece–Gould (TG) mode is quite low. Increasing electronegativity ϵ — as the density ratio between electrons and negative ions — causes a moderate increase in damping. This is largely because the free electron density decreases, which alters the plasma dielectric response and consequently changes the TG mode dispersion characteristics. Nevertheless, the massive weight and sluggish cyclotron behaviour of negative ions like SF_6^- restrict their capacity to resonate effectively with the wave field. Consequently, the energy exchange between the wave and the population of ions amorphously through cyclotron resonance is still inefficient. This inefficient wave–particle coupling quashes cyclotron damping, enabling the TG modes to sustain low attenuation and feeble interaction with the beam. As a result, beam-induced instabilities are damped in highly electronegative plasmas by virtue of the inertial dominance and weak resonant characteristics of the negative ion component.

By contrast, Figure 2 is related to the interaction of the same electron beam with a plasma with K^+ positive ions in the majority. In this case, the trend of the growth rate is very different from the above. The growth rate rises with rising k_z (cm^{-1}), and its value is considerably larger. The cause is rooted in the relatively lower mass of K^+ ions and their greater dynamic responsiveness to perturbations created by the beam. In this arrangement, the electron beam efficiently excites electrostatic Trivelpiece–Gould (TG) modes, allowing energy transfer into the plasma and the triggering of wave instabilities. A surge in electronegativity ϵ — the electron to negative ion density ratio — is shown to enhance cyclotron damping and thus inhibit instability growth. This happens due to

ISSN No. 2454-6194 | DOI: 10.51584/IJRIAS |Volume X Issue V May 2025

increased electronegativity diminishing the free electron population, which weakens collective electron-ion dynamics and degrades the requirements for robust cyclotron resonance. Consequently, resonance-mediated energy coupling between the plasma and beam diminishes, resulting in smaller instability amplitudes.

In general, the comparison highlights the prominence of ion species and electronegativity in determining beam–plasma interactions through cyclotron damping effects. Large mass and weak cyclotron sensitivity of heavy negative ions like SF_6^- result in poor coupling with TG modes, resulting in increased damping and reduction of beam-driven instabilities. Conversely, plasmas with light positive ions such as K^+ allow for stronger cyclotron resonance, enabling more effective absorption of energy from the beam and consequently diminishing damping—enabling instabilities to develop more easily. In addition, the reverse tendencies exhibited by rising electronegativity in negative versus positive ion plasmas accentuate the intricate interconnection between plasma content and wave–particle interacting dynamics. These findings are important to the stability control of electronegative plasmas and also for beam-driven plasma system design for laboratory and space applications.

Using the same equations, the growth rates for Case I (Eq. 17) and Case II (Eq. 17) have been analysed as functions of beam density n_{b0} (cm^{-3}) for various values of longitudinal wave number k_z (cm^{-1}), as shown in Figure 3 and Figure 4, respectively.

Figure 3 and Figure 4 show the electron beam density n_{b0} (cm^{-3}) dependence of the growth rate for various longitudinal wavenumbers k_z (cm^{-1}), in electronegative (and electropositive (K^+) plasmas, respectively. The first plot (Fig. 3), that of the SF_6^- plasma, shows a comparatively lower value of growth rate across the entire beam density range. The growth of Γ1 with n_{b0} (cm^{-3}) is sub-linear and gradual, and the rate of growth decreases with higher k_z (cm^{-1}). This is typical of inhibited wave growth caused by the presence of negative ions, which enhance plasma inertia and decrease overall coupling between the electron beam and plasma oscillations. On the contrary, the second plot (Fig.4) for the K^+ plasma indicates much larger growth rate for the same or even lower beam densities. The plots are more steeply increasing, indicating increased beam-plasma instability, particularly at higher k_z (cm^{-1}) values. This higher Γ2 indicates that the availability of light positive ions (K^+) enables more efficient energy transfer between the beam and the plasma, since the plasma is more responsive to perturbations without the added damping effects of heavy negative ions.

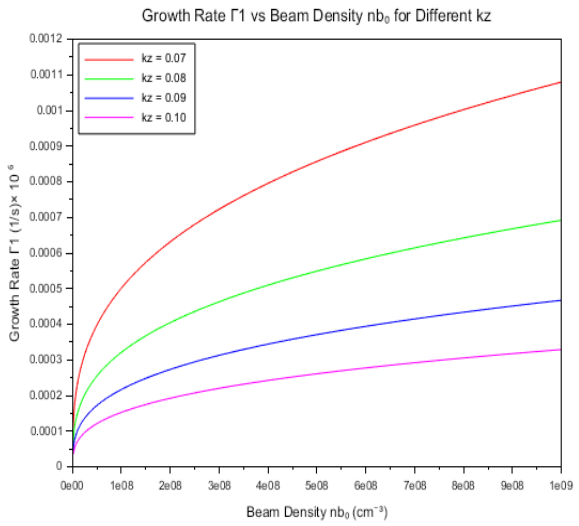

Figure 3. The figure depicts the variation in the growth rate Γ1 (s^{-1}) of the unstable TG wave mode with respect to beam density n_{b0} (cm^{-3}) for different values of longitudinal wave number k_z (cm^{-1}), in the presence of a negative ion and an electron beam

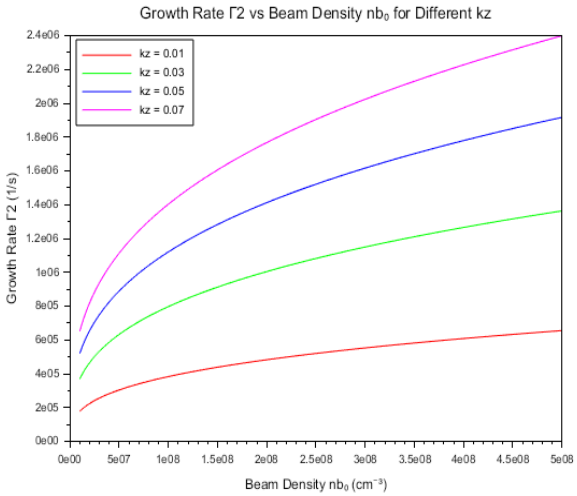

Figure 4 illustrates the variation of the growth rate Γ2 (s^{-1}) of the unstable TG wave mode with respect to beam density n_{b0} (cm^{-3}) for different values of longitudinal wave number k_z (cm^{-1}), in the presence of a positive ion and an electron beam

ISSN No. 2454-6194 | DOI: 10.51584/IJRIAS |Volume X Issue V May 2025

The striking difference in cyclotron damping behaviour of Trivelpiece–Gould modes is a result of the intrinsic ion charge polarity and mass differences. In plasmas with heavy negative ions like SF_6^-, poor wave–ion energy transfer due to the heavy ion mass and poor cyclotron resonance means cyclotron damping is very low. This weak coupling permits TG modes to propagate with minimal attenuation, in essence screening the plasma from beam-driven energy transfer. By contrast, positive ion plasmas composed of lighter species such as K^+ show stronger cyclotron resonance, permitting more efficient coupling between wave and ion motion. This leads to greater cyclotron damping, wherein wave energy is actively absorbed by the ion population.

In addition, the impact of rising axial wavenumber k_z (cm^{-1}) differs between the two cases. In SF_6^- plasmas, damping continues to be weak or even diminishes with k_z (cm^{-1}), which means higher spatial frequency TG modes remain less damped and remain predominantly undamped. On the other hand, in K^+ plasmas, cyclotron damping gets stronger with growing k_z (cm^{-1}), echoing stronger wave–ion coupling and greater efficiency in energy dissipation at shorter wavelengths. For better visualization and understanding 3-D plots representing the variation of growth rates have been given in Figures 5 and 6 corresponding to 2-D plots (Figs. 3 and 4) respectively.

This comparison is essential in planning plasma systems where controlled instability or suppression are necessary, e.g., in plasma-based accelerators, thrusters, or plasma processing environment where negative ions SF_6^- such as are deliberately introduced.

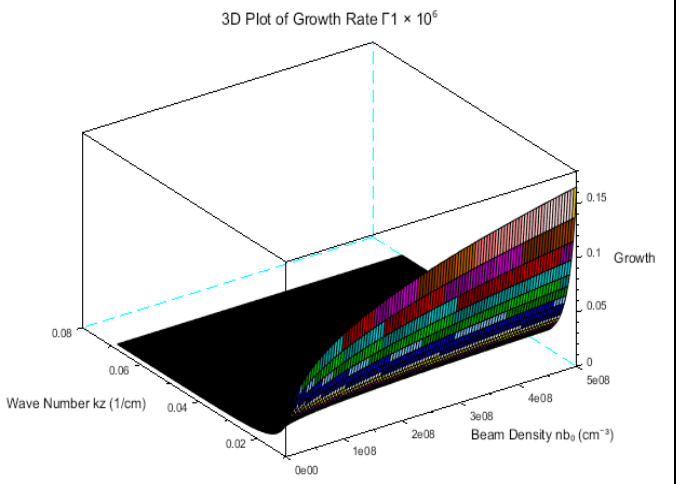

Figure 5 3-D plot showing the variation of growth rate Γ1 (sec^{-1}) of unstable mode of TG wave with respect to beam density n_{b0} (cm^{-3}) for different values k_z (cm^{-1}) in presence of negative ion and electron beam

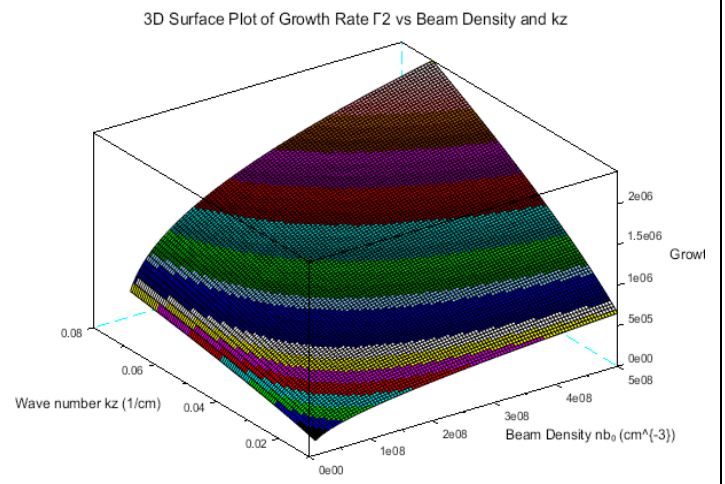

Figure 6 3-D plot showing the variation of growth rate Γ2 (sec^{-1}) of unstable mode of TG wave with respect to beam density n_{b0} (cm^{-3}) for different values k_z (cm^{-1}) in presence of positive ion and electron beam

EXPERIMENTAL AND THEORETICAL EVIDENCE SUPPORTING CYCLOTRON DAMPING BEHAVIOUR IN ELECTRONEUTRAL AND ELECTRONEGATIVE PLASMAS

Comparison of cyclotron damping characteristics of Trivelpiece–Gould (TG) modes in SF_6^- and K^+ plasmas reveals significant ion mass and charge polarity roles. In heavy negative ion dominant plasmas like SF_6^-, the weak cyclotron resonance and enhanced plasma inertia result in significantly lower damping rates of TG modes. This weak coupling allows the TG modes to travel with little attenuation and hence screen the plasma from

ISSN No. 2454-6194 | DOI: 10.51584/IJRIAS |Volume X Issue V May 2025

beam-driven energy transfer. This kind of suppression of wave excitation and damping by heavy negative ions has experimental backing in which electron beams excite ion cyclotron waves in electronegative plasmas, with observations of reduced wave-particle energy transfer caused by the heavy negative ions [34]. In the same way, experimental observation of plasma wave propagation in inductively coupled plasmas shows that adding negative ions minimizes instability growth by enhancing plasma inertia and reducing effective beam–plasma coupling [35]. In addition, the damping of beam-excited wave generation in plasmas with heavy negatively charged particles is similar to dusty plasma experimental results with negatively charged dust particles, wherein ion beam excitation of the dust acoustic wave is greatly suppressed [36].

By contrast, plasmas with lighter positive ions like K^+ have more intense cyclotron resonance, enabling improved wave–ion coupling and increased cyclotron damping. Increasing damping with increasing axial wavenumber k_z indicates more intense wave-particle interaction and greater energy dissipation efficiency at shorter wavelengths. These differences highlight the important role of plasma composition in the stability and energy processes of beam-plasma systems.

CONCLUSION

The electron beam interaction in SF_6^- and K^+ plasmas compared shows different cyclotron damping properties of Trivelpiece–Gould modes, dominated mainly by ion mass and electronegativity. For SF_6^- dominated plasmas, the heavier negative ions show weak cyclotron resonance, causing lower damping and very little energy transfer to the wave field. This produces relatively prolonged TG mode propagation with negligible attenuation. Conversely, K^+ plasmas of lighter positive ions show greater cyclotron coupling, which increases energy transfer and results in more efficient damping of TG modes. Increasing axial wavenumber k_z increases damping in K^+ plasmas, whereas damping remains weak in SF_6^- environments. These findings highlight that positive ion plasmas are more effective in wave energy damping through cyclotron mechanisms, while negative ion plasmas naturally inhibit such damping because of their inertial and resonant constraints.

REFERENCES

1. Trivelpiece, A. W., & Gould, R. W. (1959). Space charge waves in cylindrical plasma columns. Journal of Applied Physics, 30(12), 1784. https://doi.org/10.1063/1.1735053
2. Malmberg, J. H., & Wharton, C. B. (1966). Dispersion of electron plasma waves. Physical Review Letters, 17(4), 175–177. https://doi.org/10.1103/PhysRevLett.17.175
3. Mannheimer, W. M. (1969). Nonlinear development of an electron plasma wave in a cylindrical waveguide. Physics of Fluids, 12(11), 2426–2431. https://doi.org/10.1063/1.1692352
4. Lynov, J. P., Michelsen, P., Pecseli, H. L., Rasmussen, J. J., Saeki, K., & Turikov, V. A. (1979). Observations of solitary structures in a magnetized, plasma-loaded waveguide. Physica Scripta, 20(3–4), 328–333. https://doi.org/10.1088/0031-8949/20/3-4/015
5. Schamel, H. (1979). Theory of electron holes. Physica Scripta, 20(3–4), 336–342. https://doi.org/10.1088/0031-8949/20/3-4/016
6. Stenzel, R. L., & Urrutia, J. M. (2016). Trivelpiece-Gould modes in a uniform unbounded plasma. Physics of Plasmas, 23(9), 092103. https://doi.org/10.1063/1.4962269
7. Praburam, G., & Sharma, A. K. (1992). Second-harmonic excitation of a Gould-Trivelpiece mode in a beam-plasma system. Journal of Plasma Physics, 48(1), 3–15. https://doi.org/10.1017/S0022377800016402
8. Seiler, S., Yamada, M., & Ikezi, H. (1976). Lower hybrid instability driven by a spiraling ion beam. Physical Review Letters, 37(11), 700–703. https://doi.org/10.1103/PhysRevLett.37.700
9. Chang, R. P. H. (1975). Lower-hybrid beam-plasma instability. Physical Review Letters, 35(1), 28–30. https://doi.org/10.1103/PhysRevLett.35.28
10. Sharma, S. C., Srivastava, M. P., Sugawa, M., & Tripathi, V. K. (1998). Excitation of lower hybrid waves by a density-modulated electron beam in a plasma cylinder. Physics of Plasmas, 5(9), 3161–3165. https://doi.org/10.1063/1.873050
11. Prakash, V., Gupta, R., Sharma, S. C., & Vijayshri. (2013). Excitation of lower hybrid waves by an ion

beam in a magnetized plasma. Laser and Particle Beams, 31(4), 747–751. https://doi.org/10.1017/S0263034613000631
12. Pieper, J. B., & Goree, J. (1996). Dispersion of plasma dust acoustic waves in the strong coupling regime. Physical Review Letters, 77(15), 3137–3140. https://doi.org/10.1103/PhysRevLett.77.3137
13. Thompson, C., Barkan, A., D'Angelo, N., & Merlino, R. L. (1997). Dust acoustic waves in a direct current glow discharge. Physics of Plasmas, 4(6), 2331–2335. https://doi.org/10.1063/1.872453
14. Sharma, S. C., Sharma, K., & Walia, R. (2012). Ion beam driven ion-acoustic waves in a plasma cylinder with negatively charged dust grains. Physics of Plasmas, 19(7), 073706. https://doi.org/10.1063/1.4739406
15. Kaur, D., Sharma, S. C., Pandey, R. S., and Gupta, R., "Excitation of Gould–Trivelpiece mode by streaming particles in dusty plasma," Laser and Particle Beams, vol. 37, pp. 122–127, 2019, doi: 10.1017/S0263034619000284.Barkan, A., D'Angelo, N., & Merlino, R. L. (1996). Experiments on ion-acoustic waves in dusty plasmas. Planetary and Space Science, 44(3), 239–242. https://doi.org/10.1016/0032-0633(95)00129-X
16. Rosenberg, M. (1993). Ion- and dust-acoustic instabilities in dusty plasma. Planetary and Space Science, 41(3), 229–233. https://doi.org/10.1016/0032-0633(93)90002-Z
17. Annaratone, B. M., Escarguel, A., Lefevre, T., Rebont, C., Claire, N., & Doveil, F. (2011). Rotation of magnetized plasma. Physics of Plasmas, 18(3), 032108. https://doi.org/10.1063/1.3567122
18. Bettega, G., Cavaliere, F., Cavenago, M., Illiberi, A., Pozzoli, R., & Romé, M. (2005). Plasma fluctuations in a linear magnetized plasma column. Plasma Physics and Controlled Fusion, 47(12B), B577–B587. https://doi.org/10.1088/0741-3335/47/12B/S52
19. David, P. (2017). Tomography in a linear magnetized plasma (PhD thesis). Aix-Marseille Université.
20. Dem'yanov, V. G., Yeliseyev, Y. N., Kirochkin, Y. A., Luchaninov, A. A., Panchenko, V. I., & Stepanov, K. N. (1988). Equilibrium and nonlocal ion cyclotron instability of plasma in crossed longitudinal magnetic and strong radial electric fields. Soviet Journal of Plasma Physics, 14, 494–498. https://doi.org/10.1017/S002237782300137X
21. Dubin, D. H. E. (2016). Penning traps and plasma modes. In M. Knoop, N. Madsen, & R. C. Thompson (Eds.), Trapped charged particles: A graduate textbook with problems and solutions (pp. [insert page range if known]). World Scientific.
22. Fajans, J. (1993). Transient ion resonance instability. Physics of Fluids B: Plasma Physics, 5(9), 3127–3135. https://doi.org/10.1063/1.860728
23. Jaeger, S. (2010). Étude théorique et expérimentale des instabilités basses fréquences dans un plasma en champs magnétique et électrique croisés (PhD thesis). Aix-Marseille Université.
24. Kabantsev, A. A., & Driscoll, C. F. (2003). Diocotron instabilities in an electron column induced by a small fraction of transient positive ions. AIP Conference Proceedings, 692(1), 61–68. https://doi.org/10.1063/1.1622463
25. Levy, R. H., Daugherty, J. D., & Buneman, O. (1969). Ion resonance instability in grossly nonneutral plasma. Physics of Fluids, 12(12), 2616–2629. https://doi.org/10.1063/1.1692333
26. Peurrung, A. J., Notte, J., & Fajans, J. (1993). Observation of the ion resonance instability. Physical Review Letters, 70(20), 295–298. https://doi.org/10.1103/PhysRevLett.70.295
27. Sakawa, Y., & Joshi, C. (2000). Growth and nonlinear evolution of the modified Simon-Hoh instability in an electron beam-produced plasma. Physics of Plasmas, 7(5), 1774–1780. https://doi.org/10.1063/1.874012
28. Yeliseyev, Y. N. (2006). Nonlocal theory of the spectra of modified ion cyclotron oscillations in a non–neutral plasma produced by gas ionization. Plasma Physics Reports, 32(11), 927–936. https://doi.org/10.1134/S1063780X06110058
29. Yeliseyev, Y. N. (2010). Oscillation spectrum of an electron gas with a small density fraction of ions. Plasma Physics Reports, 36(7), 563–582. https://doi.org/10.1134/S1063780X10070048
30. Yeliseyev, Y. N. (2024). Trivelpiece–Gould modes and low-frequency electron–ion instability of non-neutral plasma. Journal of Plasma Physics, 90, 935900103. https://doi.org/10.1017/S002237782300137X
31. Kaur, D., Sharma, S. C., & Pandey, R. S. (2018). Excitation of a Gould-Trivelpiece (TG) mode by relativistic electron beam (REB) in magnetized dusty plasma. Journal of Atomic, Molecular, Condensate & Nano Physics, 5(2), 81–96. https://doi.org/10.26713/jamcnp.v5i2.922

32. Mikhailovski, A. B. (1974). Theory of Plasma Instabilities, Vol. 1: Instabilities of a Homogeneous Plasma. New York: Consultant Bureau.
33. Chang, R. P. H. (1975). Lower-hybrid beam-plasma instability. Physical Review Letters, 35(1), 28–30. https://doi.org/10.1103/PhysRevLett.35.28
34. Fernsler, R. F., Stenzel, R. L., & Urrutia, J. M. (2015). Electrostatic ion cyclotron waves driven by electron beams in electronegative plasmas. Physics of Plasmas, 22(3), 033503. https://doi.org/10.1063/1.4913531
35. Rauf, S., Lieberman, M. A., & Lichtenberg, A. J. (2000). Measurement and modelling of negative ion effects on plasma wave propagation and instabilities in inductively coupled plasmas. Plasma Sources Science and Technology, 9(3), 315–325. https://doi.org/10.1088/0963-0252/9/3/312
36. Sharma, S. C., Kaur, D., Gahlot, A., & Sharma, J. (2014). Excitation of dust acoustic waves by an ion beam in a plasma cylinder with negatively charged dust grains. Physics of Plasmas, 21(10), 103702. https://doi.org/10.1063/1.4897312
37. B. Song, N. D'Angelo, and R. L. Merlino, "Electrostatic waves in a dusty plasma," Phys. Fluids B: Plasma Phys., vol. 3, no. 2, pp. 284–286, 1991. DOI: 10.1063/1.859880